NASA TECHNICAL NOTE

NASA TN D-3393

NASA TN D-3393

EXPERIMENTAL INVESTIGATION OF THE THERMAL BOUNDARY LAYER IN A CONFINED LIQUID

by Michael J. Kolar

Lewis Research Center

Cleveland, Ohio

NATIONAL AERONAUTICS AND SPACE ADMINISTRATION • WASHINGTON, D. C. • APRIL 1966

EXPERIMENTAL INVESTIGATION OF THE THERMAL BOUNDARY LAYER IN A CONFINED LIQUID

By Michael J. Kolar

Lewis Research Center
Cleveland, Ohio

NATIONAL AERONAUTICS AND SPACE ADMINISTRATION

For sale by the Clearinghouse for Federal Scientific and Technical Information
Springfield, Virginia 22151 – Price $0.50

EXPERIMENTAL INVESTIGATION OF THE THERMAL BOUNDARY LAYER IN A CONFINED LIQUID

by Michael J. Kolar

Lewis Research Center

SUMMARY

The boundary layer flow in a confined liquid is studied in the case of constant heat flux. Parameters are developed to indicate the presence of both a quasi-steady state and boundary layer flow. The conditions under which mathematical similarity may exist in the boundary layer temperature and velocity fields are derived, and the coupling between the boundary layer and interior flows is discussed. Measured temperature profiles in the boundary layer exhibit similarity in a region in which startup and free surface effects are negligible. The predicted temperature profiles for a flat plate in an infinite medium agree fairly well with the measured profiles in the region where similarity exists.

INTRODUCTION

The general problem of a confined liquid subjected to a heat flux has been studied recently in connection with the heating of cryogenic propellants for rockets. In order to design propellant tanks for space vehicles properly, the behavior of the propellant flow field should be known. Small scale experiments with noncryogenic liquids have been reported in references 1 and 2, while larger scale experiments with liquid hydrogen have been reported in reference 3. An analytical solution to the momentum and energy equations governing a liquid contained in a horizontal cylinder subjected to wall heating is reported in reference 4. Numerical solutions to the Navier-Stokes equations for liquid contained in a vertical parallelepiped with heated walls are given in reference 5, which also gives an excellent bibliography on confined heated liquids. These investigations indicate that, under the heat loads usually experienced by a space vehicle during powered flight, a natural-convection boundary layer forms along the propellant tank wall, and an axial temperature gradient develops in the fluid bulk. In addition, a layer of saturated liquid forms near the surface. The analyses also show that the temperature throughout

the tank depends very slightly on the radial coordinate.

When an analytical approach is used to predict the flow field in a rocket propellant tank, a number of engineering approximations are usually made to simplify the Navier-Stokes equations. The simplifying assumptions usually proceed with the application of boundary layer theory taken from steady-state results on vertical flat plates in an infinite medium. Therefore, the approximate solutions obtained in propellant heating analyses preclude possible transient effects and ignore the coupling that exists between the boundary layer and the interior, or bulk, flow. Neglecting the transient effects is based on the concept that the fluid is in a quasi-steady state, that is, that the flow fields behave as if they were governed by the steady-state process at each instant of time. Ignoring the coupling between the boundary layer and interior flows is generally based on the argument that the propellant tank is sufficiently large so that only small changes can occur in the interior flow, and therefore, that only small changes can occur in the boundary layer as a result of the coupling. In other words, only a weak coupling exists between the boundary layer and interior flows. Under these conditions, the flow field in a completely confined fluid is replaced by free-convection flow in an infinite medium. The assumption is then made that the temperature distributions in the tank wall and in the propellant are such that the conditions of profile similarity for both the thermal and velocity boundary layers are satisfied.

The conditions for the aforementioned assumptions to be valid are neither quantitatively defined nor universally met. Thus, to satisfy the need for a more definitive description of completely confined fluids, a study was made to determine criteria under which the preceding assumptions are valid. The purpose of this study was twofold: (1) to arrive at a set of parameters that define the necessary conditions under which the simplifying assumptions can be made and (2) to verify experimentally that these conditions can be satisfied for a practical situation.

An analysis was made, which consisted of normalizing the equations which govern the flow field in a confined fluid and studying the resulting parameters. Experiments were performed in a glass tank, which enclosed a noncryogenic fluid and which was subjected to a constant wall heat flux. Experimental data were then compared with the analytical parameters that were developed.

GOVERNING PARAMETERS

The discussion that follows is based on the flow in a two-dimensional rectangular cell of liquid subjected to a constant wall heat flux (fig. 1). The fluid is considered to have a free surface on the top and thermal insulation at the bottom. It is assumed that all fluid properties are constant, and viscous dissipation and work against the body force

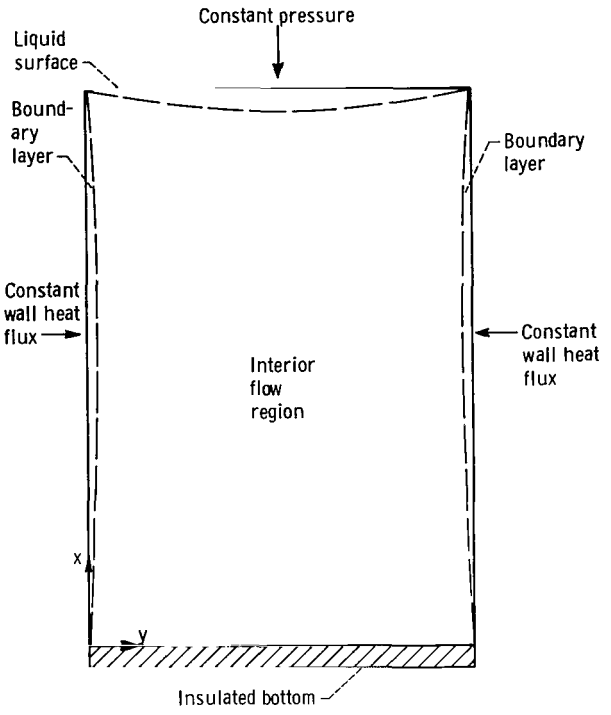

Figure 1 - Proposed model for enclosed liquid subjected to constant wall heat flux.

are neglected. Density is assumed constant except in the formation of buoyancy terms. The coordinate system is taken with the origin at one corner of the cell, x as the ordinate, and y as the abscissa. The cell is assumed symmetrical about the centerline. Only the laminar flow regime is considered.

Conservation Laws

The equations expressing conservation of mass, x- and y-components of momentum, and energy in an incompressible, two-dimensional flow field may be written as (ref. 6)

$$\frac{\partial u}{\partial x} + \frac{\partial v}{\partial y} = 0$$

$$\frac{\partial u}{\partial \tau} + u\frac{\partial u}{\partial x} + v\frac{\partial u}{\partial y} = \frac{B}{\rho} - \frac{1}{\rho}\frac{\partial p}{\partial x} + \nu\nabla^2 u$$

$$\frac{\partial v}{\partial \tau} + u\frac{\partial v}{\partial x} + v\frac{\partial v}{\partial y} = -\frac{1}{\rho}\frac{\partial p}{\partial y} + \nu\nabla^2 v$$

field and wall conditions proceeds as though a steady state process exists at each instant of time. Therefore, in order for a quasi-steady state to exist, the time derivatives in equations (3a) and (3b) must be negligible. This implies that the term $\left(L^2/\nu\tau_0\right)(Pr/Ra)^{1/2}$ must be small. In order to evaluate this term, a characteristic time τ_0, which is related to the boundary conditions, must be chosen. Gebhart (ref. 7) shows that, for a vertical flat plate in an infinite medium, the characteristic time τ_0 can be taken as

$$\tau_0 = \frac{L^2}{\alpha}(bRa^*)^{-2/5} \tag{6}$$

where b is a function of Pr, and Ra* is the modified Rayleigh number. This same characteristic time may be associated with the problem of a confined fluid, since the wall temperature rise leads all other temperature rises in the system, and the rate of wall temperature rise is at least as great as the rate of rise of any other temperature in the system. The use of equation (6) produces the following condition under which a quasi-steady state may exist:

$$\frac{(PrRa)^{1/2}}{(bRa^*)^{2/5}} \gg 1 \tag{7}$$

Similarity Solution of Boundary Layer Equations

It is assumed that a constant wall heat flux is imposed on a confined fluid in such a manner that a boundary layer flow exists and the system is in a quasi-steady state. If the interior temperature is of a certain form, the boundary layer temperature and velocity profiles can be shown to exhibit the property of similarity. However, the interior temperature cannot be obtained directly from a solution of the interior equations, since no boundary conditions exist to govern these equations. Solutions for the boundary layer flow field can be generated if the interior equations are used to provide boundary conditions for the boundary layer equations. It has been shown in reference 5 that, in the interior of the fluid, $\partial T/\partial y \approx 0$. If this relation is used in the interior equations, it follows that $\partial\psi/\partial y \approx 0$. Therefore, the following set of approximate boundary conditions can be written for the quasi-steady boundary layer equations:

$$\left.\begin{aligned} &\left.\begin{aligned} &\frac{\partial \psi}{\partial y} = \frac{\partial \psi}{\partial x} = 0 \\ &q_w = -k \left.\frac{\partial T}{\partial y}\right|_w \end{aligned}\right\} y = 0,\ 0 \le x \le L \\ &\left.\begin{aligned} &\frac{\partial \psi}{\partial y} = 0 \\ &T = T_B(x) \end{aligned}\right\} y = \infty,\ 0 < x << L \end{aligned}\right\} \tag{8}$$

The assumption that $\partial T/\partial y \approx 0$ in the interior flow does not hold both near the liquid surface, where high values of the radial gradient have been observed, and near the tank bottom, where the boundary layer assumptions are invalid.

It is possible to impose an artificial condition on the boundary layer equations by replacing the term ΔT by the term $T(x) - T_B(x)$. (Note that the interior temperature T_B is assumed to depend on x only.) This leads to the following partial differential equations for the laminar boundary layer flow of a confined fluid in a quasi-steady state:

$$\left(\frac{\partial \psi}{\partial y}\frac{\partial}{\partial x} - \frac{\partial \psi}{\partial x}\frac{\partial}{\partial y}\right)\frac{\partial \psi}{\partial y} = f\beta(T - T_B) + \nu \frac{\partial^3 \psi}{\partial y^3} \tag{9a}$$

$$\left(\frac{\partial \psi}{\partial y}\frac{\partial}{\partial x} - \frac{\partial \psi}{\partial x}\frac{\partial}{\partial y}\right)T = \alpha \frac{\partial^2 T}{\partial y^2} \tag{9b}$$

For the case of constant wall flux, the following similarity transformation may be performed on these equations. Let an independent variable be defined by

$$\eta = \left(\frac{Gr_x^*}{5}\right)^{1/5} \frac{y}{x} \tag{10}$$

where Gr_x^* is the modified Grashof number.

New dependent velocity and temperature variables, F and θ, respectively, are defined by

$$F(\eta) = \frac{\psi}{5^{4/5}\nu\left(Gr_x^*\right)^{1/5}} \tag{11}$$

$$\theta(\eta) = \frac{k}{xq_w}\left(\frac{Gr_x^*}{5}\right)^{1/5}(T_B - T) \tag{12}$$

Applying the similarity relations (10), (11), and (12) to equations (9a) and (9b) results in the following set of ordinary differential equations:

$$F''' + 4FF'' - 3F'^2 - \theta = 0 \tag{13a}$$

$$\theta'' + Pr\left[4\theta'F - (K_1 + \theta)F'\right] = 0 \tag{13b}$$

where the primes denote differentiation with respect to η. These equations hold only if the interior temperature is of the form

$$T_B(x) = T_\infty + AK_1x^{1/5} \tag{14}$$

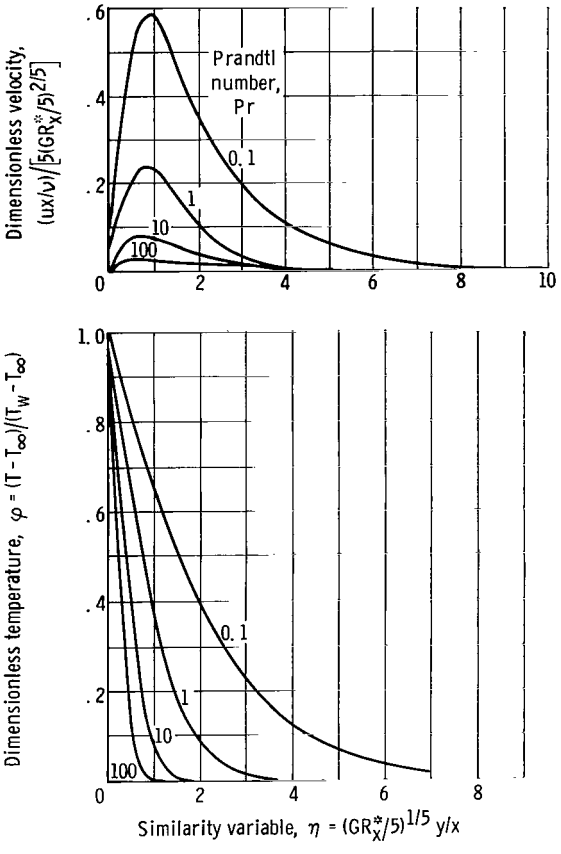

Figure 2. - Dimensionless velocity and temperature distributions in boundary layer for flat plate in infinite medium (ref. 8).

where A and K_1 are constants. For the present case of constant wall heat flux, $A = \left[\left(5\nu^2q_w^4\right)/\left(f\beta k^4\right)\right]^{1/5}$.

The boundary conditions governing equations (13a) and (13b) now become

$$\left.\begin{aligned} F &= 0 \\ F' &= 0 \\ \theta' &= 0 \end{aligned}\right\}\eta = 0 \qquad \left.\begin{aligned} F' &= 0 \\ \theta &= 0 \end{aligned}\right\}\eta = \infty \tag{15}$$

Equations (13a) and (13b) are coupled ordinary differential equations with Pr and K_1 as parameters. Numerical solutions to these equations have been given in reference 8 for the case of $K_1 = 0$. The velocity and temperature profiles in the boundary layer for this case are shown in figure 2. These profiles

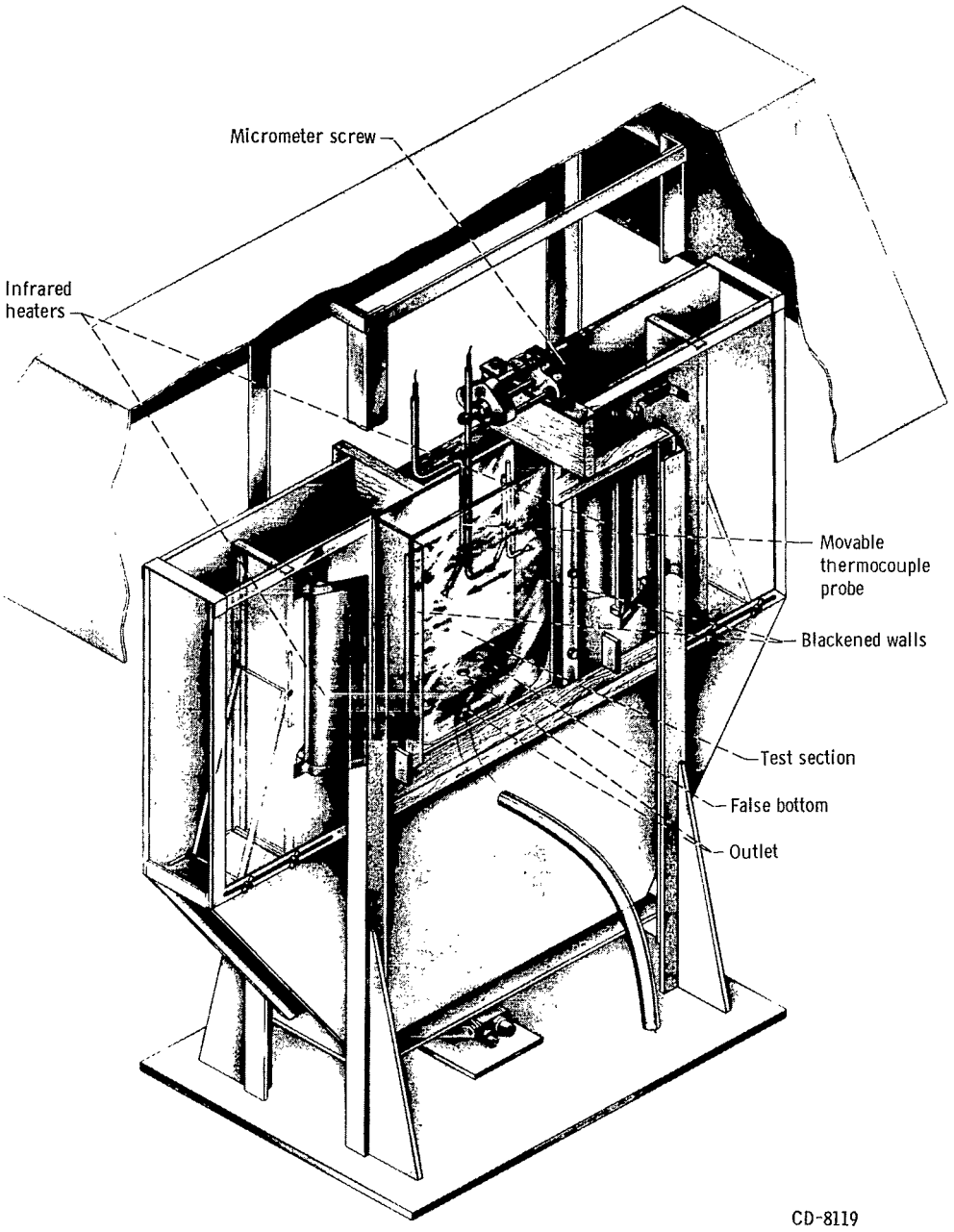

Figure 3. - Test apparatus for measurement of boundary layer temperatures.

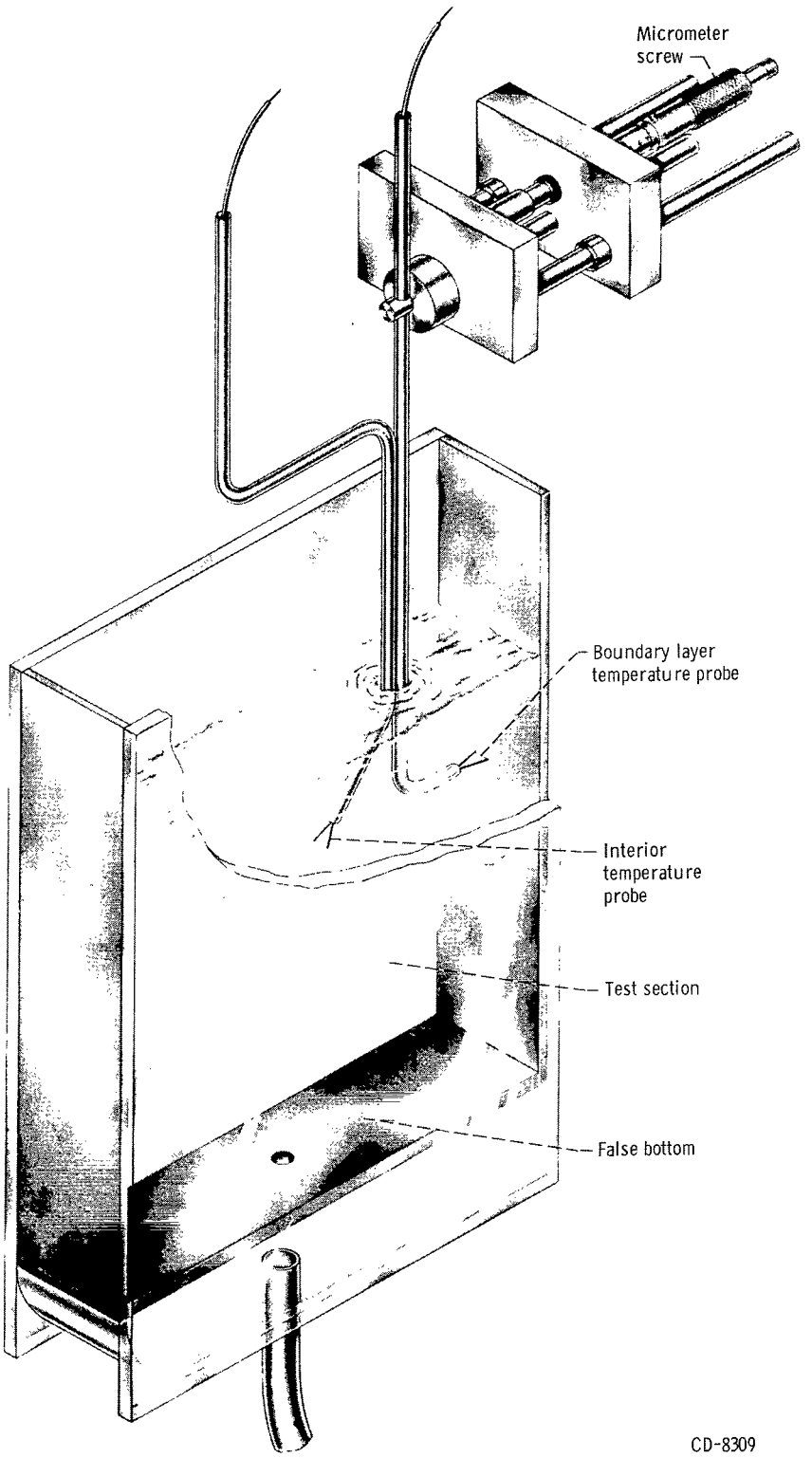

Figure 4. - Test section and probe.

depend only on η for a given Pr; that is, the profiles exhibit the property of similarity. The case $K_1 = 0$ is the usual starting point for approximate propellant heating analyses.

APPARATUS AND PROCEDURE

A cutaway view of the test rig used for measuring boundary layer and interior temperatures is shown in figure 3. With the exception of the test section, the rig was the same as that used for the experiments discussed in reference 1. The test section (fig. 4) was a rectangular-parallelepiped glass tank with inside dimensions of 20.3 centimeters wide by 30.5 centimeters high by 5.08 centimeters deep. The walls and bottom were fabricated from 0.3175-centimeter heat-resistant glass plate. A false bottom of phenolic resin (5.08 cm by 20.3 cm by 0.635 cm) was located 3.81 centimeters from the bottom of the test section and provided a definite starting place for sidewall heating. An outlet was located at the center of the bottom and false bottom plates. The top of the tank was open to permit the insertion of instrumentation. The sides of the test section from the false bottom to the top were painted black, while the bottom and the sides between the bottom and the false bottom were covered with heat-reflecting tape. The faces were clear to permit visual observations.

Cylindrical infrared lamps, 30.5 centimeters long by 0.952 centimeter in diameter, were mounted in parabolic reflectors parallel to the blackened walls. The lamps provided a wall heat flux that was proportional to the variable lamp power.

The test fluid was a 2 to 1 mixture by volume of 1, 1, 1-trichloroethane and ethyl alcohol. Table I summarizes the physical properties of these liquids and of the plate glass. Appendix B presents the method employed to obtain the thermal conductivity of the test liquid. An epoxy resin was used to cement the pieces of the test section together.

Boundary layer temperature profiles were measured with two 0.00508-centimeter (2-mil) diameter copper-constantan thermocouples; a micrometer screw was used to position the temperature probe. The movable probe is shown in two positions in figure 3, one near the wall and the other on the tank centerline. Figure 4 shows a closeup view of the test tank and probe. Two automatic recording potentiometers were employed for all temperature measurements.

Past experience had shown that end effects at the faces of the tank were negligible, as were the radial temperature gradients. Therefore, the tank acted as a two-dimensional test section, and only centerline and boundary layer temperatures were measured. Centerline temperatures were measured with a rake which consisted of a 0.952-centimeter-diameter by 30.5-centimeter-long phenolic resin rod. Copper-constantan thermocouples were mounted in 1.27-centimeter intervals starting at one end of the rod. The thermocouples extended 0.3175 centimeter from the rod.

TABLE I. - PROPERTIES OF TEST MATERIALS

Material	Density, ρ,		Specific heat, c_p,		Viscosity, μ,		Volume expansivity, β,		Thermal conductivity, k,		Prandtl number, Pr, $\frac{c_p \mu}{k}$, dimensionless
	$\frac{kg}{cu\ m}$	$\frac{lb\ mass}{cu\ ft}$	$\frac{J}{(kg)(^oC)}$	$\frac{Btu}{(lb\ mass)(^oF)}$	$\frac{(N)(sec)}{sq\ m}$	$\frac{lb\ mass}{(hr)(ft)}$	$\frac{1}{^oC}$	$\frac{1}{^oF}$	$\frac{J}{(sec)(m)(^oC)}$	$\frac{Btu}{(hr)(ft)(^oF)}$	
Ethyl alcohol (C_2H_5OH)	7.669×10^2	0.478×10^2	2.782×10^3	0.665	7.4×10^{-4}	1.81	1.065×10^{-3}	0.592×10^{-3}	0.1547	0.0895	13.3
1,1,1-Trichloroethane (CH_3CCl_3)	1.300	.812	1.075	.257	6.0	1.464	1.533	.852	------	------	----
[a]Solution of two parts 1,1,1-trichloroethane and one part ethyl alcohol	1.122	.701	1.461	.349	6.4	1.578	1.377	.765	[b].0634	.0367	15.0
Heat-resistant glass	-----	-----	-----	-----	---	-----	-----	-----	1.1311	.654	----

[a]Ref. 9 was used to calculate properties of the mixture when applicable.

[b]See appendix B.

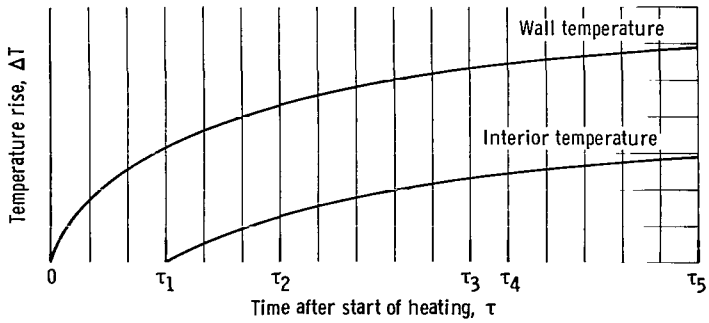

Figure 5. - Qualitative plot of temperature rise as function of time for wall and interior temperatures. Period during which system is in non-quasi-steady state, 0 to τ_1; time interior temperature begins to rise, τ_1; for $\tau > \tau_1$ system is in quasi-steady state; average time during which first set of boundary layer temperatures is measured, $(\tau_2 + \tau_3)/2 = \tau_{a1}$; average time during which second set of boundary layer temperatures is measured, $(\tau_4 + \tau_5)/2 = \tau_{a2}$.

To measure temperature profiles near the wall, the temperature probe (see fig. 4) was positioned with one thermocouple in contact with the wall and the other approximately 3 centimeters from the wall. The tank was filled to a height of 12.7 centimeters, and power was applied to the infrared lamps, which were then permitted to operate for approximately 180 seconds before data were taken. Temperature readings were then taken simultaneously with both thermocouples, as the probe was moved in 0.00254-centimeter (1-mil) increments away from the wall. The temperature recorded by the thermocouple farthest from the wall was used as the temperature in the interior of the fluid $T_B(x)$.

A qualitative plot of the wall and interior temperatures as functions of time is shown in figure 5. The wall temperature increases rapidly at first and the system is in a non-steady state. At some time $\tau = \tau_1$, the interior temperature begins to rise, and the system approaches a quasi-steady state. Boundary layer temperature measurements were made at times greater than τ_1. Obviously, the measurements for a given value of x and q_w extended over some period of time, for example, τ_2 to τ_3. The average time after the start of heating τ_a during the measurement is given by $(\tau_2 + \tau_3)/2$. If a second measurement of the boundary layer temperature profile is made during a later time interval τ_4 to τ_5, the average time after the start of heating is given by $(\tau_4 + \tau_5)/2$ for this measurement.

To measure the wall heat flux produced by the lamps, a second test tank was constructed with thermocouples embedded on both sides of one wall. This test tank was identical to that used in reference 1 and is shown schematically in figure 6. This figure also shows the instrumented wall with the 16 copper-constantan thermocouples in place; the thermocouples were positioned opposite each other, 8 on either side of the wall. The inner thermocouples (those nearest the liquid) were mounted by drilling at an angle through the glass wall from the outside, inserting the thermocouple, and filling the remaining space with an epoxy resin. The outer thermocouples were positioned on the

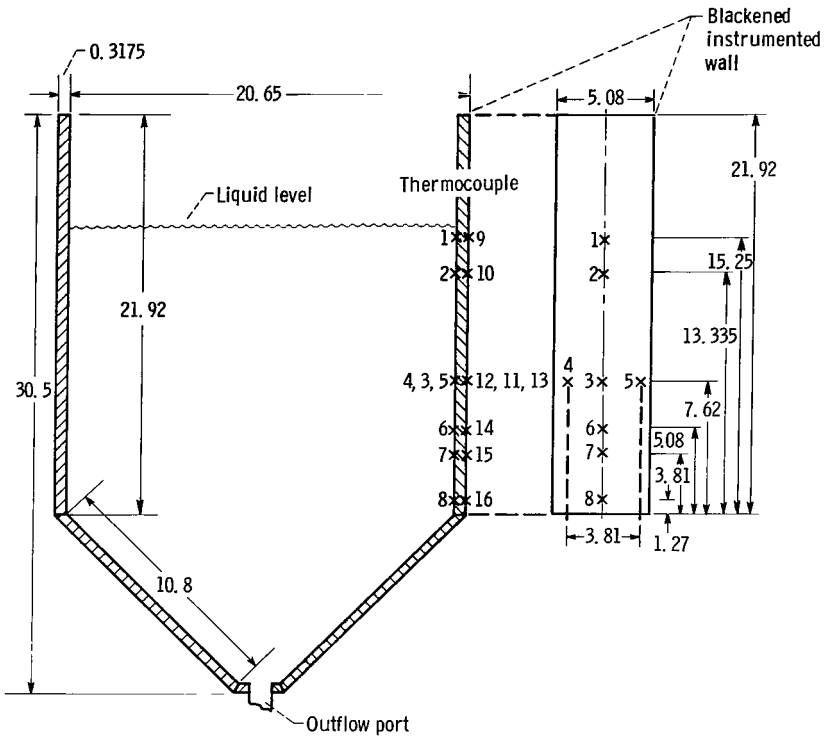

Figure 6. - Test section with instrumented wall for measuring wall heat flux. (All dimensions in centimeters.)

glass and held in place with epoxy. A small sheet of metal was placed over, but not in contact with, each of the outer thermocouples to prevent direct absorption of the radiation. The outside wall was then painted black. Temperature gradients through the wall were measured at six positions for two values of lamp power. The heat flux q_w was then calculated from the equation

$$q_w = -k_g \frac{\Delta T}{\Delta Y}$$

where ΔY is the wall thickness (0.3175 cm) and ΔT is the temperature difference across the wall. It was assumed that the wall temperature could be approximated as a linear function of Y. An experimentally determined relation between the lamp power P and the wall heat flux was found to be $q_{w,1}/q_{w,2} = P_1/P_2$, where the subscripts denote different values of applied lamp voltage.

Figure 7 presents a plot of q_w at six positions on the wall for a value of P of 256 watts. Data are presented in 60-second intervals up to a maximum of 480 seconds after the start of heating. It can be seen that q_w rises rapidly for 180 seconds and then remains fairly constant at any position. There were, however, differences between the values of q_w measured at the various positions for a given time. These deviations were

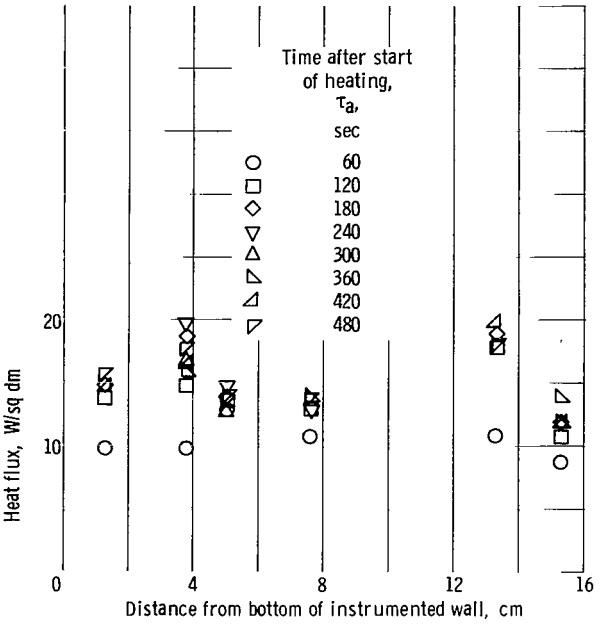

Figure 7. - Measured wall heat flux imposed by infrared lamps. Applied lamp power, 256 watts.

TABLE II. - AVERAGE VALUES OF WALL HEAT FLUX

[Lamp power = 256 W.]

Time after start of heating, τ, sec	Average wall heat flux, q_w,	
	W/sq dm	Btu/(hr)(sq in.)
60	10.89	2.40
120	13.39	2.95
180	14.25	3.14
240	14.48	3.19
300	13.62	3.00
360	13.89	3.06
420	14.11	3.11
480	14.61	3.22

caused by two experimental problems: first, the thermocouples were mounted with epoxy that could not be made uniformly thick; and, second, the lamps did not give a completely uniform distribution.

The six values of q_w were then arithmetically averaged for each time increment, and the average values are presented in table II. It can be seen that the average wall heat flux rises rapidly for 180 seconds and then remains fairly constant in time. Since all boundary layer temperatures were measured after at least 180 seconds of heating, the average of the average values of q_w after 180 seconds was used as the value of q_w. For P equal to 256 watts, q_w is 14.16 watts per square decimeter (3.12 Btu/(hr)(sq in.).

The values of wall heat flux used in this experiment were chosen to give laminar boundary layer flow, which exists for values of Gr_x up to 10^9. Under this restriction, three values of q_w were decided on, such that an arbitrary factor of 3 separated the maximum and minimum values.

RESULTS AND DISCUSSION

The underlying motive of these experiments was to determine whether boundary layer temperature profiles can be predicted by the similarity approach discussed in the analysis. The important parameter was found to be K_1, which describes the coupling between the interior and bulk temperatures. The region of interest was that part of the flow field

which was sufficiently far from the bottom and the liquid surface so that geometrical and free surface effects could be neglected.

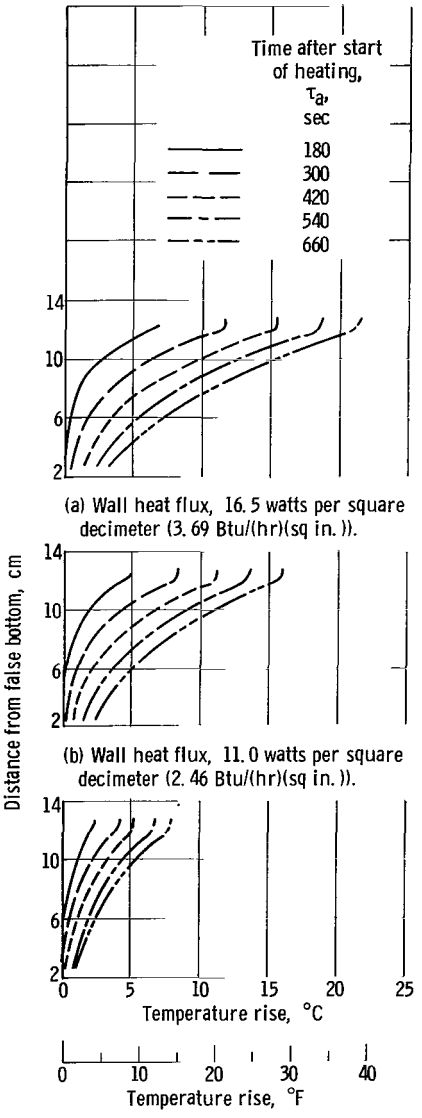

(a) Wall heat flux, 16.5 watts per square decimeter (3.69 Btu/(hr)(sq in.)).

(b) Wall heat flux, 11.0 watts per square decimeter (2.46 Btu/(hr)(sq in.)).

(c) Wall heat flux, 5.5 watts per square decimeter (1.23 Btu/(hr)(sq in.)).

Figure 8. - Centerline temperature profile with time after start of heating as parameter. Liquid level, 12.7 centimeters.

Temperature Measurements

Fluid temperatures taken on the central tank axis are presented in figure 8 for three values of q_w, 5.5, 11.0, and 16.5 watts per square decimeter (1.21, 2.42, and 3.63 Btu/(hr)(sq in.)), for times after the start of heating of 180, 300, 420, 540, and 660 seconds. Each of the profiles can be represented approximately by a function of the form

$$T_B(x) = T_\infty + K_2 x^{3/2} \tag{16}$$

Radial temperature profiles taken near a heated wall are presented in figure 9. Both wall heating and the boundary layer are assumed to start at the false bottom of the test section; therefore, the origin of the coordinate system is at the junction of the tank wall and the false bottom. Since measurements start at two times after the start of heating (see fig. 5, p. 13) for each value of x and since measurement of a single profile extends over a time interval of about 200 seconds, the average time after the start of heating τ_a is used to characterize each profile. Temperature distributions are given in terms of the following nondimensional variables:

$$\varphi = \frac{T(x) - T_B(x)}{T_w(x) - T_B(x)}$$

$$\eta = \left(\frac{Gr_x^*}{5}\right)^{1/5} \frac{y}{x}$$

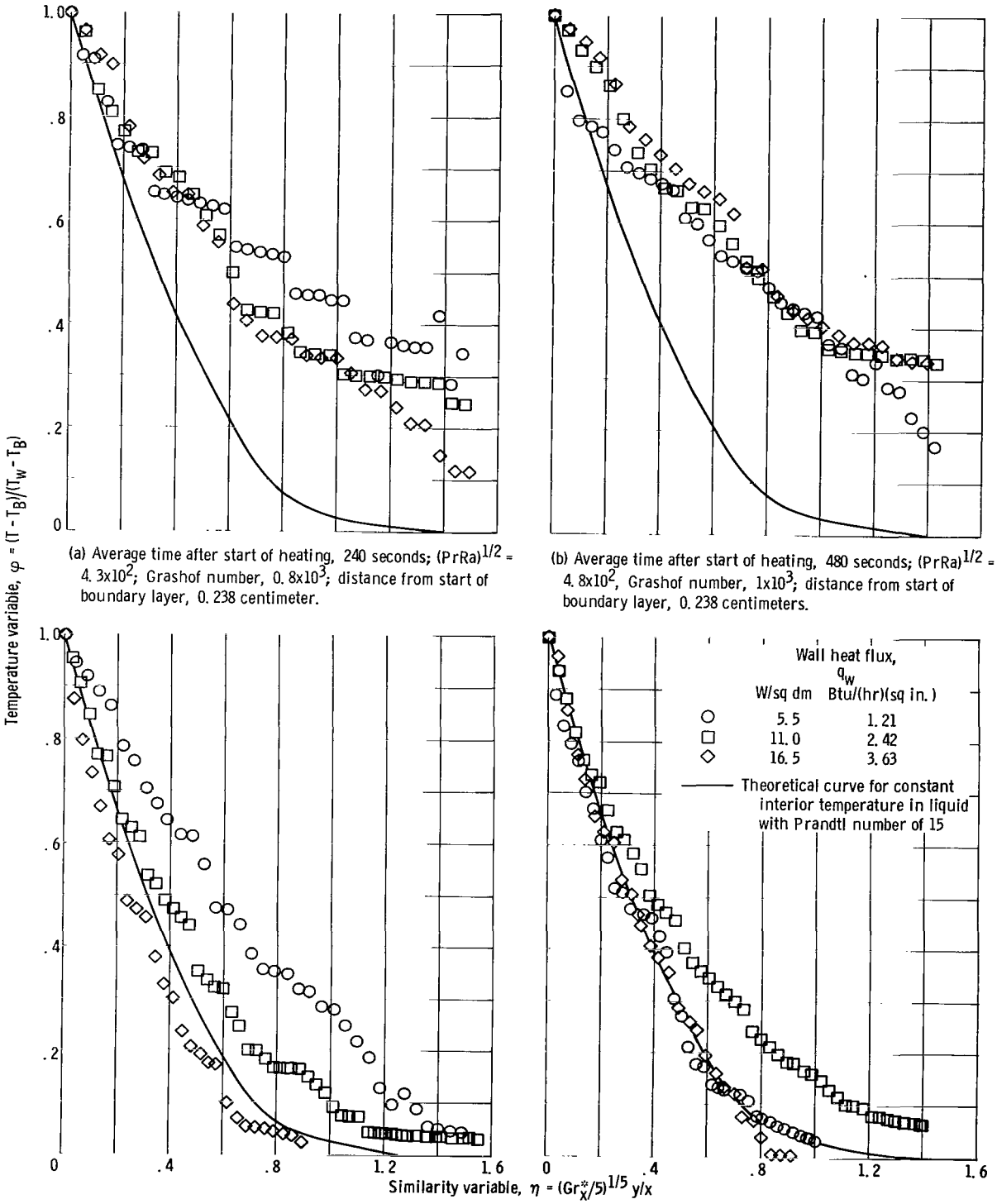

(a) Average time after start of heating, 240 seconds; $(PrRa)^{1/2} = 4.3 \times 10^2$; Grashof number, 0.8×10^3; distance from start of boundary layer, 0.238 centimeter.

(b) Average time after start of heating, 480 seconds; $(PrRa)^{1/2} = 4.8 \times 10^2$, Grashof number, 1×10^3; distance from start of boundary layer, 0.238 centimeters.

(c) Average time after start of heating, 240 seconds; $(PrRa)^{1/2} = 2.1 \times 10^4$, Grashof number, 2×10^6; distance from start of boundary layer, 2.54 centimeters.

(d) Average time after start of heating, 480 seconds; $(PrRa)^{1/2} = 2.3 \times 10^4$, Grashof number, 2.4×10^6; distance from start of boundary layer, 2.54 centimeters.

Figure 9. - Measured temperature distributions near heated wall with wall heat flux as parameter.

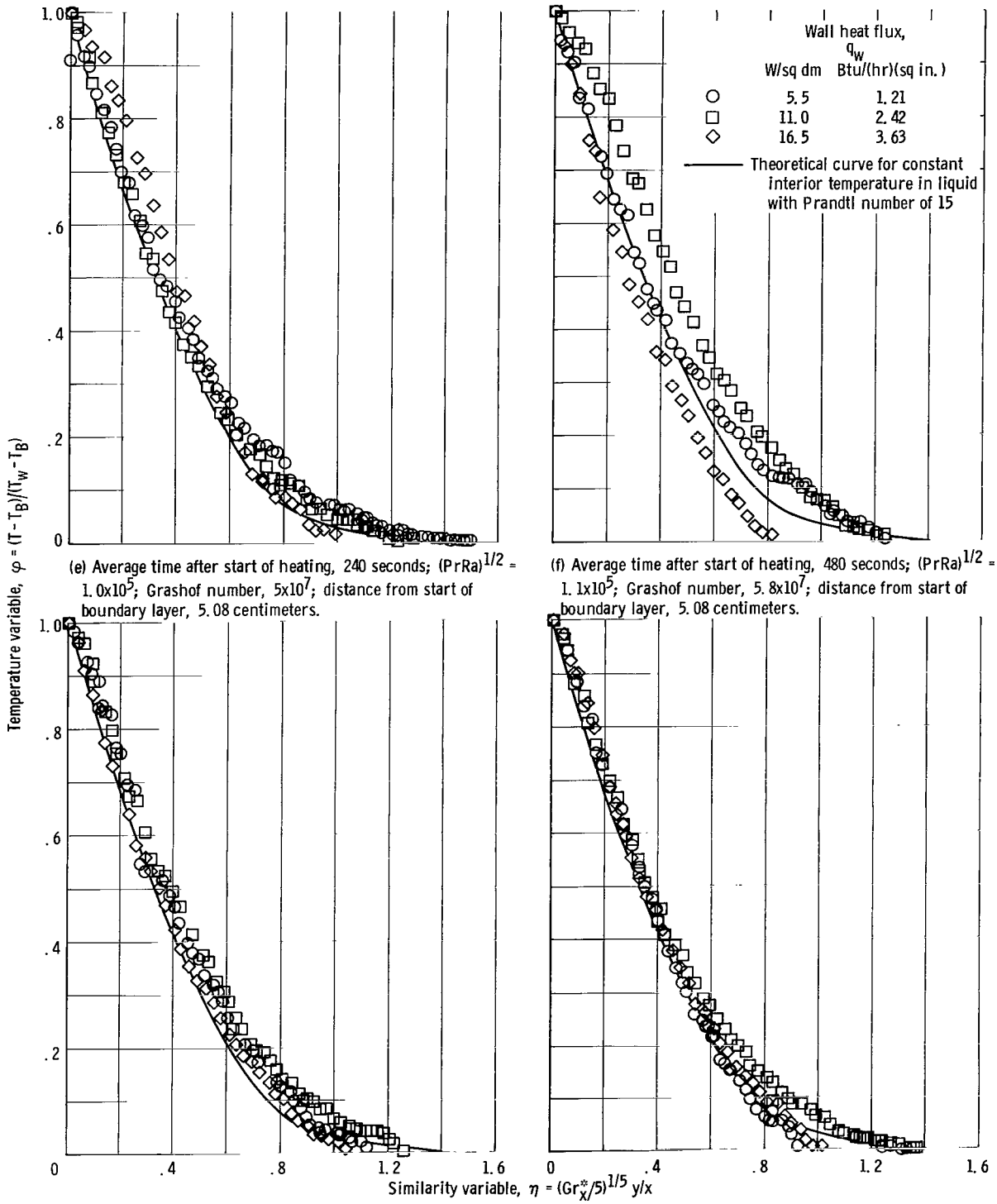

(e) Average time after start of heating, 240 seconds; $(PrRa)^{1/2} = 1.0 \times 10^5$; Grashof number, 5×10^7; distance from start of boundary layer, 5.08 centimeters.

(f) Average time after start of heating, 480 seconds; $(PrRa)^{1/2} = 1.1 \times 10^5$; Grashof number, 5.8×10^7; distance from start of boundary layer, 5.08 centimeters.

(g) Average time after start of heating, 240 seconds, $(PrRa)^{1/2} = 2.4 \times 10^5$; Grashof number, 2.5×10^8; distance from start of boundary layer, 7.62 centimeters.

(h) Average time after start of heating, 480 seconds, $(PrRa)^{1/2} = 2.3 \times 10^5$; Grashof number, 2.3×10^8; distance from start of boundary layer, 7.62 centimeters.

Figure 9. - Continued.

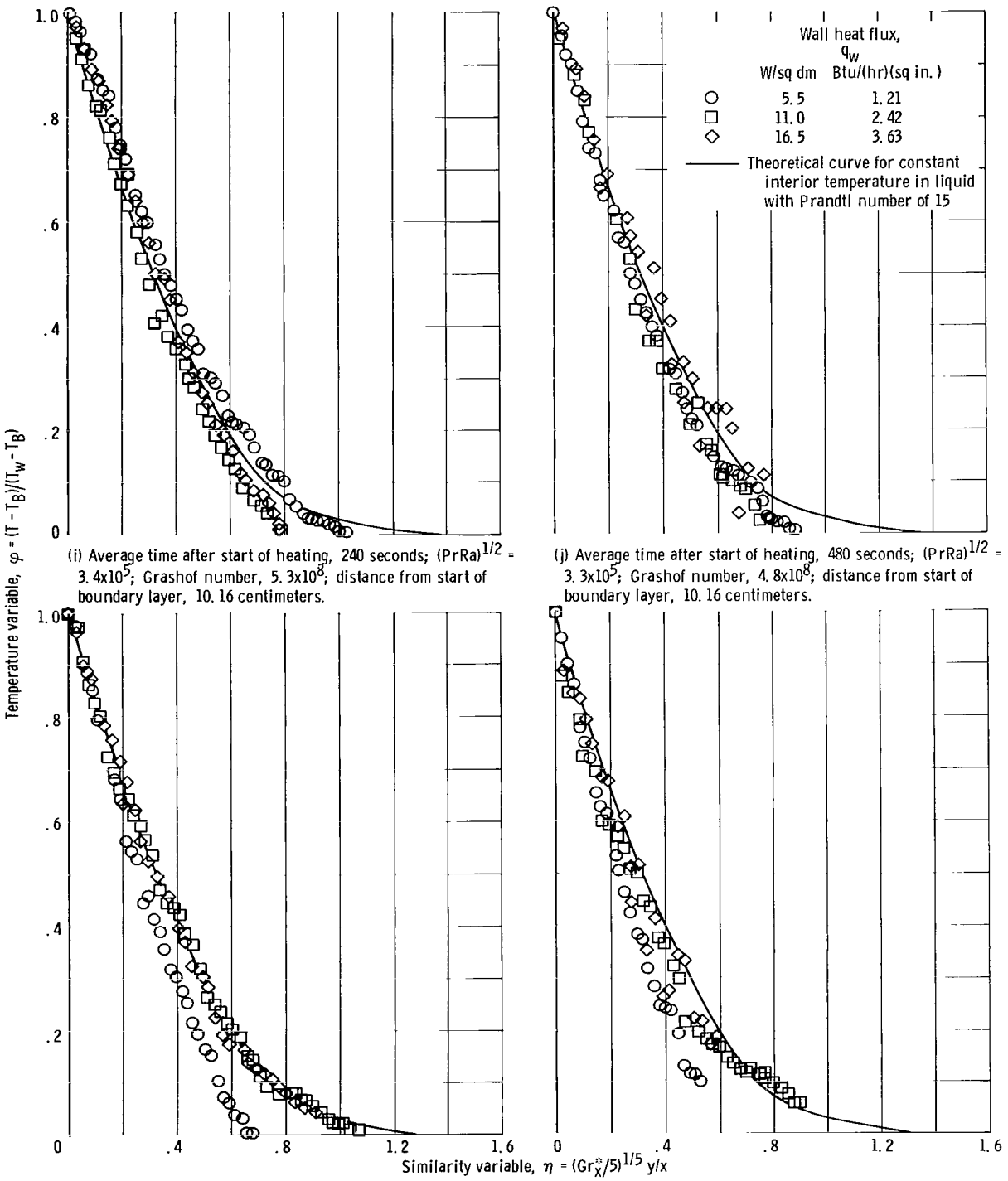

(i) Average time after start of heating, 240 seconds; $(PrRa)^{1/2} = 3.4 \times 10^5$; Grashof number, 5.3×10^8; distance from start of boundary layer, 10.16 centimeters.

(j) Average time after start of heating, 480 seconds; $(PrRa)^{1/2} = 3.3 \times 10^5$; Grashof number, 4.8×10^8; distance from start of boundary layer, 10.16 centimeters.

(k) Average time after start of heating, 240 seconds; $(PrRa)^{1/2} = 2.5 \times 10^5$; Grashof number, 2.7×10^8; distance from start of boundary layer, 11.43 centimeters.

(l) Average time after start of heating, 480 seconds; $(PrRa)^{1/2} = 2.4 \times 10^5$; Grashof number, 2.6×10^8; distance from start of boundary layer, 11.43 centimeters.

Figure 9. – Continued.

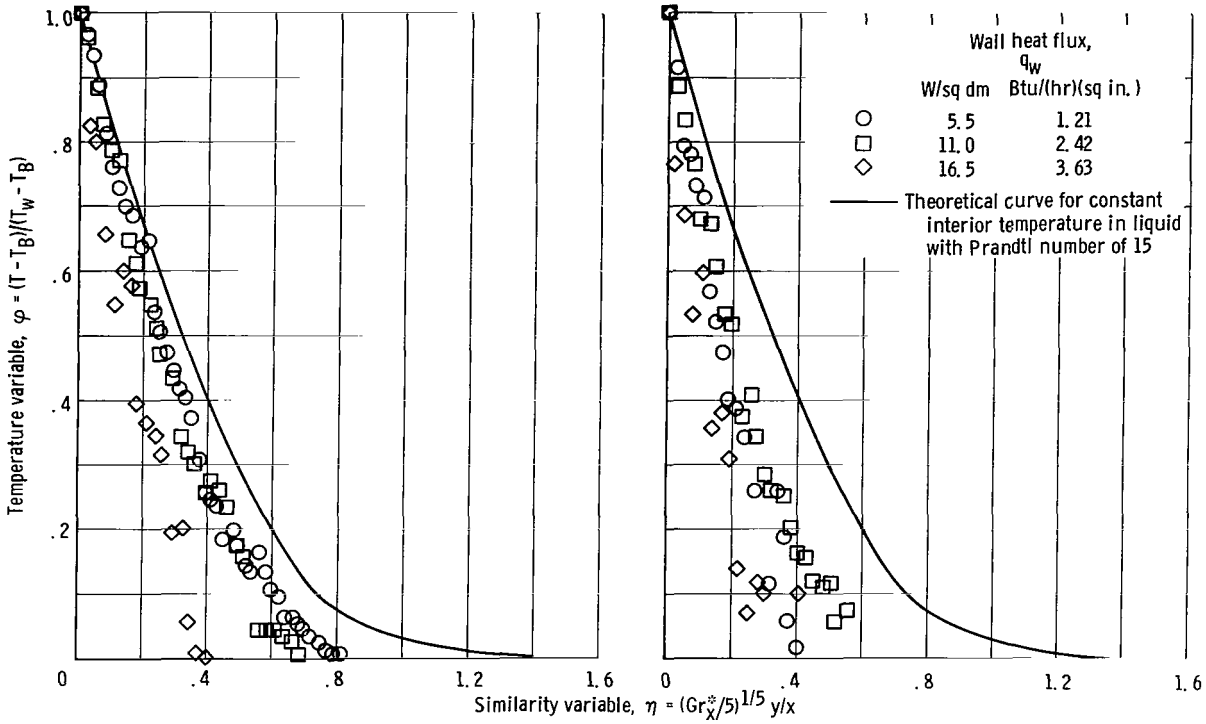

(m) Average time after start of heating, 240 seconds; $(PrRa)^{1/2} = 2.6 \times 10^5$; Grashof number, 3×10^8; distance from start of boundary layer, 12.065 centimeters.

(n) Average time after start of heating, 480 seconds; $(PrRa)^{1/2} = 2.53 \times 10^5$; Grashof number, 2.9×10^8; distance from start of boundary layer, 12.065 centimeters.

Figure 9. - Concluded.

The temperature distributions with q_w as a parameter are presented in figure 9. Distributions are given for two values of τ_a, 240 and 480 seconds. As was shown in the section GOVERNING PARAMETERS, boundary layer flow exists along the wall when the Rayleigh number is large or when $(PrRa)^{1/2} >> 1$. This quantity is given in each figure and indicates when boundary layer flow exists. The local Grashof number Gr_x gives an indication of the flow regime within the boundary layer. The boundary layer flow is laminar for Grashof numbers up to 10^9, and, as can be seen from the plots, all the data fall in this regime. In each case, the theoretical profile obtained from reference 8 for constant interior temperature is shown along with the data.

Temperature profiles for an x of 0.238 centimeter (figs. 9(a) and (b)) show poor agreement with theory. This behavior is expected since the theoretical curve was derived by using the boundary layer assumptions and, therefore, is not valid near the start of the boundary layer. Figures 9(c) to (f) present the profiles for values of x of 2.54 and 5.08 centimeters. Although there is considerable scatter in the data, experiment and theory appear to agree. The scatter is probably due to the small differences between the wall and bulk temperatures in this region and the inability of the experimental system to distinguish these differences accurately. The data for values of x of 7.62, 10.16,

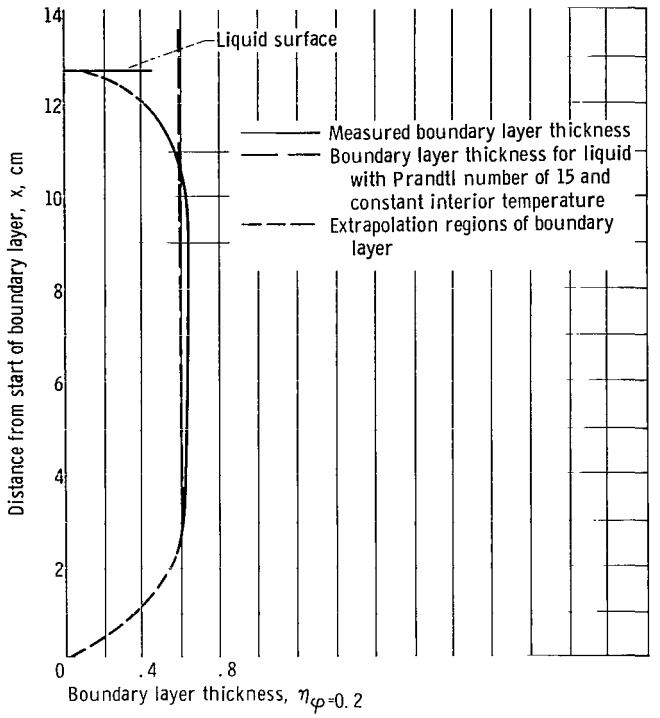

Figure 10. - Comparison of measured boundary layer shape with that predicted for liquid with constant interior temperature.

and 11.43 centimeters (figs. 9(g) to (ℓ)) agree very well with the theoretical profiles for η near zero. However, the experimental values of φ drop to zero at lower values of η than do the theoretical values; this effect becomes greater with increasing x. The profiles for x of 12.065 centimeters are shown in figures 9(m) and (n). For this case, φ drops to zero very quickly and there is only poor agreement between theory and data even for values of η near zero.

Boundary Layer Characteristics

For purposes of this report, the thickness of the temperature boundary layer will be defined as the value of η when φ has a value of 0.2. Figure 10 shows the shape of the boundary layer as determined from the data of figure 9. Also shown in the figure is a sketch of the boundary layer along a flat plate in an infinite medium (constant interior temperature). As x increases, the effects of stratification and the liquid surface become predominant, and the experimental boundary layer thickness approaches zero near the liquid surface.

Heat is transferred from the walls to the interior of the fluid through the boundary layer. Therefore, the heat transfer coefficient between the wall and the boundary layer is useful in calculating interior temperature rises. As shown in the section GOVERNING PARAMETERS (see eq. (3c)), the local Nusselt number can be used to represent the local heat transfer coefficient. Figure 11 presents the experimental variation of Nu_x with the modified Grashof number Gr_x^* along with the theoretical variation for a flat plate in an infinite medium. The modified Grashof number Gr_x^* is used as a measure of boundary layer length and is not indicative of the wall condition. The agreement between theory and data is quite good for values of x up to and including 10.16 centimeters. This is reasonable since the slope of the boundary layer temperature profile evaluated at the wall determines Nu_x, and it was indicated in the discussion of the temperature measurements that the experimental data and the theoretical curves agree quite well at $\eta = 0$. For values of x of 11.43 and 12.065 centimeters, Nu_x is much larger than predicted because of the influence of the liquid surface.

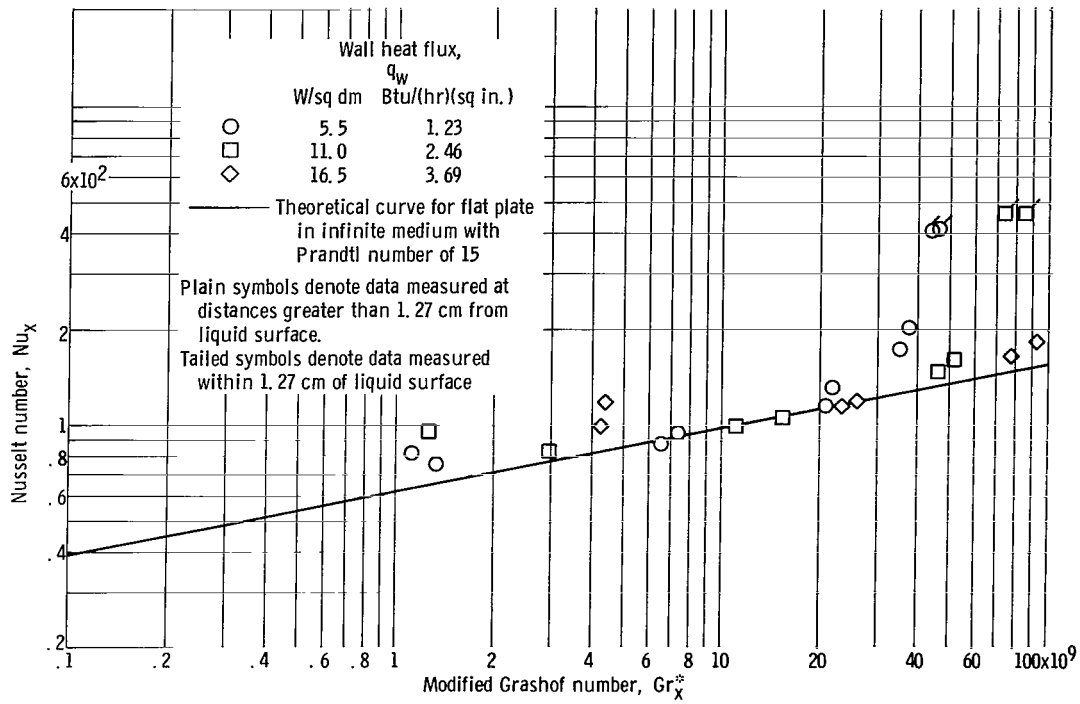

Figure 11. - Comparison of experimental data with predicted variation of Nusselt number with modified Grashof number.

Comparison of Data With Analysis

The condition for quasi-steady operation (eq. (7)) depends, through the Rayleigh number, on the difference between the wall and interior temperatures at a given axial height. After 180 seconds of operation, this temperature difference was found to be nearly constant; that is, the wall and interior temperatures rise at approximately the same rate. Table III shows the average temperature difference between the wall and interior, along with the value of the quasi-steady state term $(PrRa)^{1/2}(bRa^*)^{-2/5}$, after 240 and 480 seconds of operation for each value of heat flux employed. The maximum value of x is used to evaluate the quasi-steady

TABLE III. - EXPERIMENTAL PARAMETERS FOR QUASI-STEADY OPERATION

Wall heat flux, q_w, W/sq dm	Average time after start of heating, τ_a, sec	Average difference between wall and bulk temperatures, ΔT_o, ^oC	Quasi-steady state term, $\frac{(PrRa)^{1/2}}{(bRa^*)^{2/5}}$
5.5	240	4.64	53.3
5.5	480	4.43	52.0
11.0	240	7.16	50.0
11.0	480	7.16	50.0
16.5	240	9.06	48.0
16.5	480	8.00	45.1

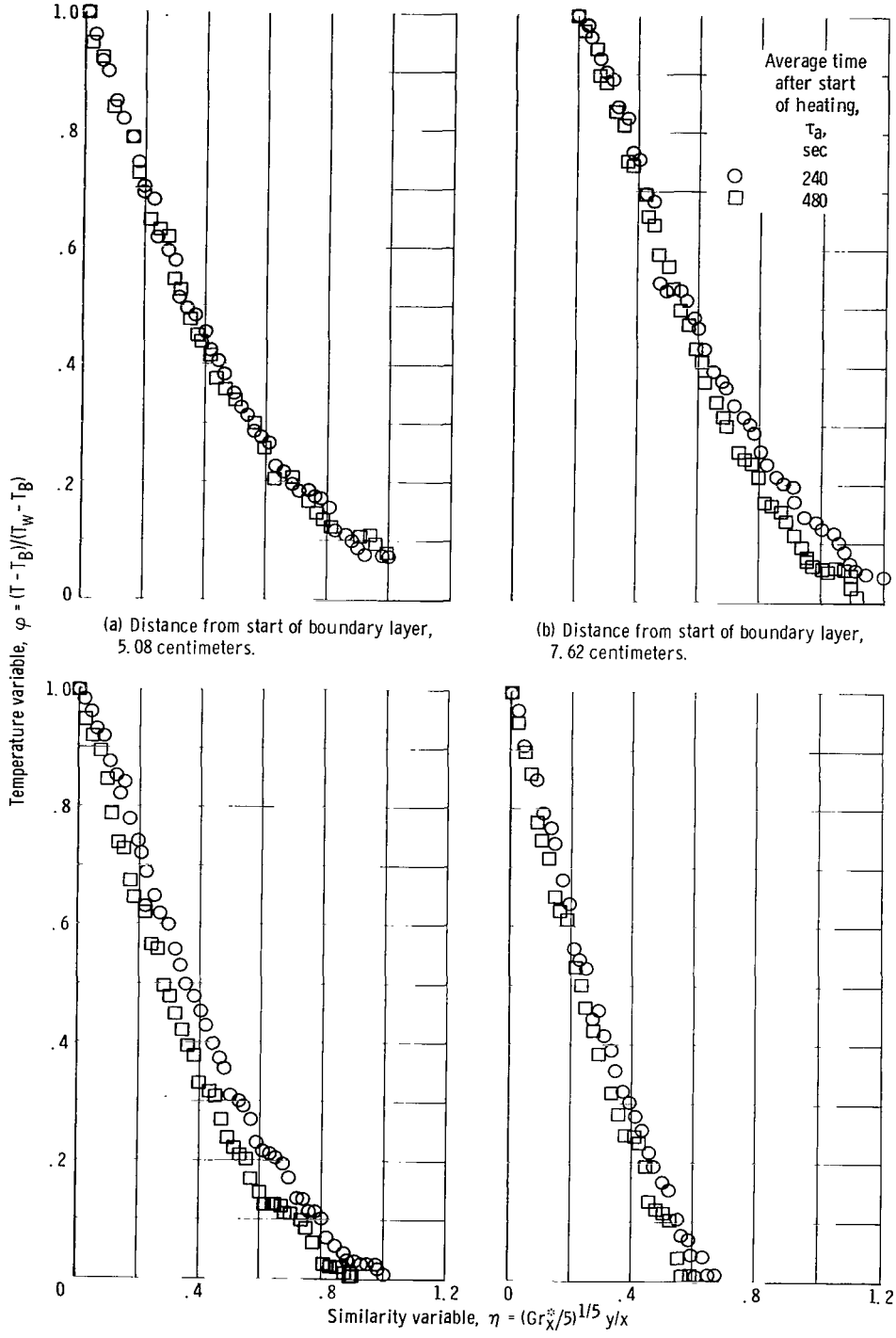

(a) Distance from start of boundary layer, 5.08 centimeters.

(b) Distance from start of boundary layer, 7.62 centimeters.

(c) Distance from start of boundary layer, 10.16 centimeters.

(d) Distance from start of boundary layer, 11.43 centimeters.

Figure 12. - Measured temperature distributions near heated wall with average time after start of heating as parameter. Wall heat flux, 5.5 watts per square decimeter.

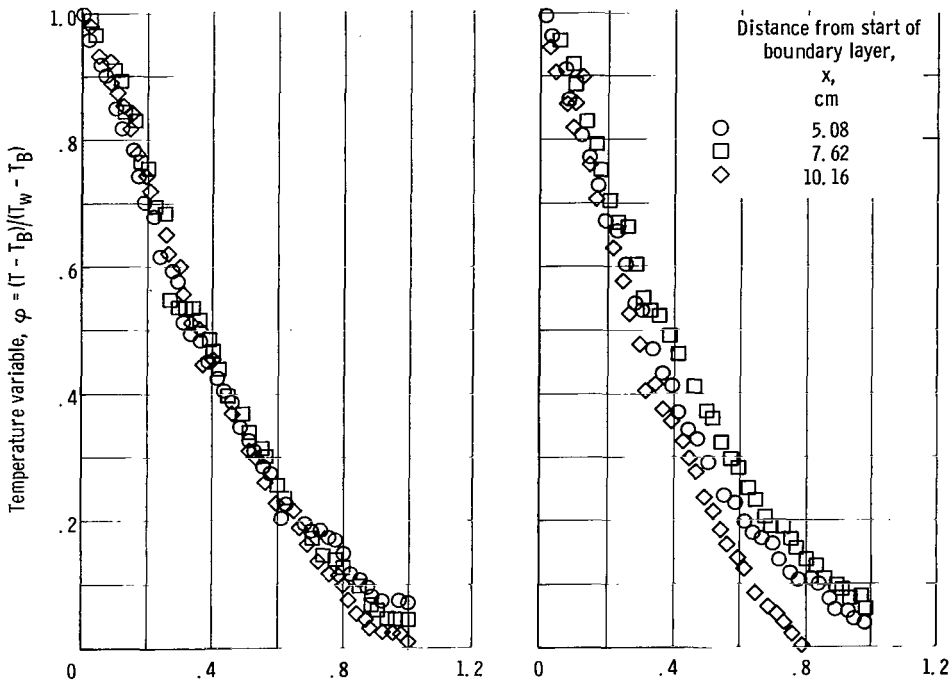

(a) Wall heat flux, 5.5 watts per square decimeter.

(b) Wall heat flux, 11.0 watts per square decimeter

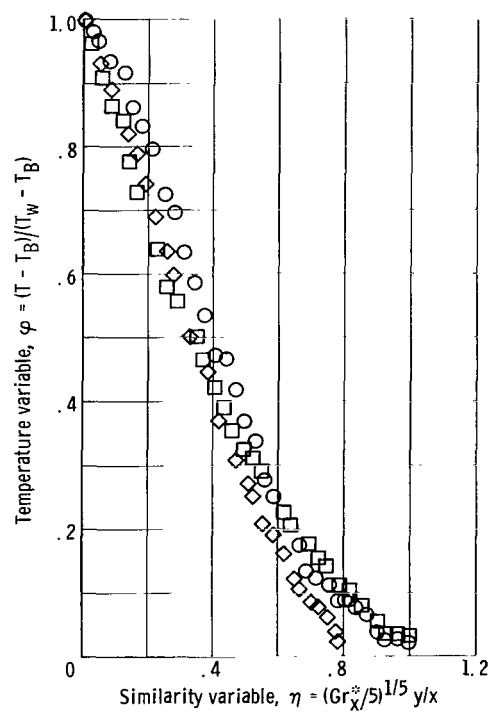

(c) Wall heat flux, 16.5 watts per square decimeter.

Figure 13. - Measured temperature distribution near heated wall with distance from start of boundary layer as parameter. Average time after start of heating, 240 seconds.

condition, since this condition depends on $x^{-1/10}$. The results show that a quasi-steady state existed for values of τ_a of 240 and 480 seconds.

The temperature profiles in the boundary layer possess the property of similarity if they depend only on the similarity variable η for a given heat flux. Figure 12 shows measured boundary layer temperature profiles for a q_w of 5.5 watts per square decimeter with τ_a as a parameter for values of x of 5.08, 7.62, 10.16, and 11.43 centimeters. The data are independent of τ_a for these values of x. The same behavior was noted for the values of q_w not shown in figure 12.

Profiles with x as a parameter are presented in figure 13. Data are presented for a q_w of 5.5, 11.0, and 16.5 watts per square decimeter for a τ_a of 240 seconds. The data indicate that the profiles are approximately independent of x for x-values of 5.08, 7.62, and 10.16 centimeters. This is true, even though $T_B(x)$ is not of the required form. The nondependence of the profiles on τ_a and x between 5.08 and 10.43 centimeters indicates that the concept of similarity can be used in this region.

For values of x greater than 10.43 centimeters, similarity does not exist. The apparent cause is that the liquid surface perturbs the boundary layer flow and destroys similarity characteristics in this region. This perturbation is reflected in the local Grashof numbers, which decrease for values of x greater than 10.43 centimeters (see figs. 9(k) to (n)); this effect indicates that the difference between the wall and interior temperatures is decreasing as the surface is approached.

Equation (13b) shows that the interior and boundary layer temperatures are coupled through the parameter K_1. This equation predicts that the boundary layer temperature profiles will possess the characteristic of similarity provided that the interior temperature is of the form shown in equation (14). Equation (13b) also shows that the boundary layer temperature profiles will be nearly identical to those for constant interior temperature if $K_1 \ll |\theta(\eta)|$. It has been found experimentally that the interior temperature is not of the required form (see eq. (16)). Nevertheless, the boundary layer temperature profiles appear to be similar in certain regions of the boundary layer, and the profiles for $K_1 = 0$ give a good approximation of the data. It is of interest to express these ideas in a quantitative manner.

Since the experimental boundary layer temperature profiles exhibit similarity to some degree, it can be assumed that the interior temperature profile is of the required form. This means that

$$AK_1x^{1/5} = K_2x^{3/2} \tag{17}$$

Because A and K_2 are assumed to be constants, this equation infers that K_1 is actually a function of x. To find an explicit form for $K_1(x/L)$, divide both sides of equation (17) by L and solve for K_1. Then,

$$K_1 = K_2 L^{13/10} \left(\frac{x}{L}\right)^{13/10} A^{-1} \tag{18}$$

Since K_1 is a function of x, the boundary layer profiles cannot be truly similar, and it was noted earlier in this section that the profiles were only approximately independent of x. The slight x dependence was most obvious for $\eta >> 0$. Now $\theta(\eta)$ has a maximum absolute value when $\eta = 0$ and approaches a value of zero as $\eta \to \infty$, that is, in the interior of the fluid. Assume that $K_1 << |\theta(0)|$. Then, as η increases, a point is reached at which $K_1 = |\theta(\eta_1)|$. In the region near η_1, the profiles cannot be similar. The positive ratio $K_1/[-\theta(\eta)]$ can be formed by using equations (12) and (17). Then,

$$\frac{K_1(x)}{-\theta(\eta)} = \frac{1}{\frac{\Delta T}{\Delta T_B} - 1} \tag{19}$$

Therefore, $K_1(x) = |\theta(\eta_1)|$ when $\Delta T = 2\,\Delta T_B$. In plotting the data, the parameter $\varphi(\eta)$ given by $\varphi = \theta(\eta)/\theta(0)$ was used. Then $\varphi(\eta_1)$ can be found by setting $\Delta T = 2\,\Delta T_B$ and

$$\varphi(\eta_1) = 2\,\Delta T_B - \frac{\Delta T_B}{\Delta T_W - \Delta T_B}$$

or

$$\varphi(\eta_1) = \frac{1}{\frac{\Delta T_W}{\Delta T_B} - 1} \tag{20}$$

This equation is somewhat ambiguous because ΔT_W and ΔT_B change with η. However, values of these quantities when, for example, $\eta = 1.0$ can be used to provide a close approximation for $\varphi(\eta_1)$. For the system under consideration, it was found that $\Delta T_W >> \Delta T_B$ when $\eta = 1.0$, and from equation (20), $\varphi(\eta_1)$ is nearly zero. This agrees with the observation that the profiles are similar when φ is near 1.0, but similarity is less evident as φ approaches zero.

To make the foregoing discussion more concrete, consider the case where $q_w = 16.5$ watts per square decimeter and $\tau = 660$ seconds (fig. 8, p. 16). For this case, $\Delta T_B = 0.40\, x^{3/2}$. Then $K_2 = 0.40$, $A = 88.79$, and $L^{13/10} = 0.0685$ in the mks system

of units. A few values of $K_1(x/L)$ as calculated from equation (18) would be $x/L = 0.2$ and $K_1 = 6\times10^{-5}$, $x/L = 0.5$ and $K_1 = 1.5\times10^{-4}$, and $x/L = 1.0$ and $K_1 = 3\times10^{-4}$. Thus, K_1 is of the order of 10^{-4} for the case being considered. When equation (12) and the measured temperature difference $T_B - T_W$ are used, $\theta(0)$ is of the order of 5×10^{-1} for those values of x/L where similarity was observed. Furthermore, η_1 is very close to 1.0 for this case, and $\theta(\eta_1)$ is of the order of 10^{-4}.

CONCLUDING REMARKS

The analysis and experimental results show that under the conditions studied, that is, for constant wall heat flux on a confined liquid of Prandtl number 15, the following are true:

1. The flow fields are in a quasi-steady state when the relation $(PrRa)^{1/2}(bRa^*)^{-2/5} \gg 1$ is satisfied.

2. There is a region in the laminar boundary layer in which the temperature profiles exhibit the property of similarity and are predicted fairly well by the infinite medium, flat plate model.

3. There is a region in the boundary layer near the liquid surface in which surface effects destroy similarity characteristics and reduce the boundary layer thickness.

4. The coupling between the boundary layer and interior temperature profiles is weak if $\left[K_1/\left|\theta(0)\right|\right] \ll 1$.

(The foregoing conclusions are based on the assumption that boundary layer flow exists when $(PrRa)^{1/2} \gg 1$.)

These conclusions, however, are based on temperature profiles only. To complete the study of the laminar boundary layer in a confined liquid, velocity measurements should also be obtained. Furthermore, the transition and turbulent regimes ($Gr_x > 10^9$) must be investigated in order to obtain a complete understanding of the boundary layer in an enclosed liquid.

Lewis Research Center,
National Aeronautics and Space Administration,
Cleveland, Ohio, January 19, 1966.

APPENDIX A

SYMBOLS

A	constant, $\left(5\nu^2 q_w^4 / f\beta k^4\right)^{1/5}$
B	body force per unit volume, N/cu m
b	constant, 0.0090 for liquid with Prandtl number of 15
c_p	specific heat, J/(kg)(^oC)
D	viscous dissipation function
F	similarity function for velocity
f	body force, N
Gr_x	Grashof number based on x, $(x^3 f\beta\, \Delta T)/\nu^2$, dimensionless
Gr_x^*	modified Grashof number based on x, $\left(f\beta q_w x^4\right)/k\nu^2$, dimensionless
h	heat transfer coefficient, J/(sec)(m)^2(^oC)
K_1	function describing coupling between boundary layer and interior flows
K_2	constant
k	thermal conductivity of test fluid, J/(sec)(m)(^oC)
k_g	thermal conductivity of heat resistant glass, J/(sec)(m)(^oC)
L	liquid level, used as characteristic length, cm
Nu_x	Nusselt number, (hx)/k, dimensionless
P	lamp power, W
Pr	Prandtl number, ν/α, dimensionless
p	pressure, N/sq m
p_0	reference pressure, N/sq m
q_w	wall heat flux, W/sq dm
Ra	Rayleigh number, $Gr_x Pr$, dimensionless
Ra*	modified Rayleigh number, $Gr_x^* Pr$, dimensionless
T	temperature, ^oC
T_B	bulk temperature, function of x, ^oC
T_∞	constant reference temperature, ^oC
ΔT	$T - T_\infty$, ^oC
ΔT_0	reference temperature, ^oC
u	x-component of boundary layer velocity, cm/sec
v	y-component of boundary layer velocity, cm/sec
x	coordinate parallel to heated wall, cm
ΔY	wall thickness, cm
y	coordinate perpendicular to heated wall, cm
α	thermal diffusivity, $k/\rho c_p$, sq m/sec
β	volume expansivity, $1/^oC$

η similarity variable

θ similarity function of temperature

ϑ dimensionless temperature variable, $\Delta T/\Delta T_0$

μ viscosity, N(sec)/sq m

ν kinematic viscosity, μ/ρ, sq m/sec

ρ density, kg/cu m

τ time, sec

τ_a average time after start of heating, sec

τ_0 characteristic time, sec

φ temperature variable, $[T(x) - T_B(x)]/[T_w(x) - T_B(x)]$, dimensionless

ψ stream function, sq m/sec

Subscripts:

i interior

w wall

APPENDIX B

CALCULATION OF THERMAL CONDUCTIVITY OF TEST FLUID

The following definitions are made:

k_1 thermal conductivity of ethyl alcohol

k_2 thermal conductivity of trichloroethane

k_{21} thermal conductivity of test fluid (2 to 1 mixture by volume of 1, 1, 1-trichloroethane and ethyl alcohol)

k_g thermal conductivity of heat resistant plate glass

Although a fair amount of data exists on the values of k_1 and k_g, no data could be found for the value of k_2. Furthermore, there is no universally acceptable way of predicting the thermal conductivity of an organic liquid or of a mixture of organic liquids. Consequently, the following scheme was devised for the calculation of k_{21}.

The heat flux at the heated wall is given by the relations

$$q_w = -k_g \left.\frac{\partial T}{\partial y}\right|_{w_g}$$

$$q_w = -k_{21} \left.\frac{\partial T}{\partial y}\right|_{w_{21}}$$

where the subscripts indicate that the temperature gradient must be measured in the glass or in the liquid. It will be noted that q_w was calculated in the section APPARATUS AND PROCEDURE by using the first of the aforementioned two relations. Furthermore, $\left.\frac{\partial T}{\partial y}\right|_{w_{21}}$ was measured directly. With these data, k_{21} was obtained from the relation

$$k_{21} = -\frac{q_w}{\left.\frac{\partial T}{\partial y}\right|_{w_{21}}}$$

Since k_{21} is a function of T, values of k_{21} were calculated for each value of q_w and τ_a used for the three values of x of 5.08, 7.62, and 10.43 centimeters. All values

obtained in this manner were then arithmetically averaged to give k_{21} for this set of experiments. Table IV gives the k_{21} calculated in this manner.

TABLE IV. - CALCULATED VALUES OF

THERMAL CONDUCTIVITY

[Average k_{21} = 0.0634 J/(sec)(m)(^{o}C) = 0.0367 Btu/(hr)(ft)(^{o}F).]

Wall heat flux, q_w, W/sq dm	Time after start of heating, sec	Distance from start of boundary layer, x, cm	Thermal conductivity, k_{21}, J/(sec)(m)(^{o}C)	Thermal conductivity, k_{21}, Btu/(hr)(ft)(^{o}F)
5.5	240	5.08	0.0667	0.0386
		7.62	.0759	.0439
		10.16	.0764	.0442
5.5	480	5.08	0.0574	0.0332
		7.62	.0622	.0360
		10.16	.0511	.0296
11.0	240	5.08	0.0669	0.0387
		7.62	.0657	.0380
		10.16	.0537	.0311
11.0	480	7.62	0.0584	0.0338
		10.16	.0586	.0339
16.5	240	7.62	0.0551	0.0319
		10.16	.0733	.0424
16.5	480	5.08	0.0655	0.0379
		7.62	.0624	.0361
		10.16	.0665	.0385

REFERENCES

1. Anderson, Bernhard H.; and Kolar, Michael J.: Experimental Investigation of the Behavior of a Confined Fluid Subjected to Nonuniform Source and Wall Heating. NASA TN D-2079, 1963.
2. Schwind, R. G.; and Vliet, G. C.: Observations and Interpretations of Natural Convection and Stratification in Vessels. Proceedings of the 1964 Heat Transfer and Fluid Mechanics Institute, W. H. Giedt and S. Levy, eds., Stanford University Press, 1964, pp. 51-68.
3. Huntley, Sidney C.; Gauntner, James W.; and Anderson, Bernhard H.: Wall and Bottom Heating of Liquid Hydrogen in a Propellant Tank. NASA TN D-3256, 1966.
4. Weinbaum, Sheldon: Natural Convection in a Horizontal Circular Cylinder. J. Fluid Mech., vol. 18, pt. 3, Mar. 1964, pp. 409-437.
5. Clark, J. A.: A Review of Pressurization, Stratification and Interfacial Phenomena. Vol. 10 of Advances in Cryogenic Engineering, K. D. Timmerhaus, ed., Plenum Press, 1965, Sec. M-U, pp. 259-283.
6. Schlichting, Hermann (J. Kestin, trans.): Boundary Layer Theory, McGraw-Hill Book Co., Inc., 1955.
7. Gebhart, B.; and Adams, D. E.: Measurements of Transient Natural Convection on Flat Vertical Surfaces, J. Heat Transfer, vol. 85, no. 1, Feb. 1963, pp. 25-28.
8. Sparrow, E. M.; and Gregg, J. L.: Laminar Free Convection From a Vertical Plate with Uniform Surface Heat Flux, ASME Trans., vol. 78, 1956, pp. 435-440.
9. Reid, Robert C.; and Sherwood, Thomas K.: The Properties of Gases and Liquids, McGraw-Hill Book Co., Inc., 1958.

"The aeronautical and space activities of the United States shall be conducted so as to contribute . . . to the expansion of human knowledge of phenomena in the atmosphere and space. The Administration shall provide for the widest practicable and appropriate dissemination of information concerning its activities and the results thereof."

—NATIONAL AERONAUTICS AND SPACE ACT OF 1958

NASA SCIENTIFIC AND TECHNICAL PUBLICATIONS

TECHNICAL REPORTS: Scientific and technical information considered important, complete, and a lasting contribution to existing knowledge.

TECHNICAL NOTES: Information less broad in scope but nevertheless of importance as a contribution to existing knowledge.

TECHNICAL MEMORANDUMS: Information receiving limited distribution because of preliminary data, security classification, or other reasons.

CONTRACTOR REPORTS: Technical information generated in connection with a NASA contract or grant and released under NASA auspices.

TECHNICAL TRANSLATIONS: Information published in a foreign language considered to merit NASA distribution in English.

TECHNICAL REPRINTS: Information derived from NASA activities and initially published in the form of journal articles.

SPECIAL PUBLICATIONS: Information derived from or of value to NASA activities but not necessarily reporting the results of individual NASA-programmed scientific efforts. Publications include conference proceedings, monographs, data compilations, handbooks, sourcebooks, and special bibliographies.

Details on the availability of these publications may be obtained from:

SCIENTIFIC AND TECHNICAL INFORMATION DIVISION

NATIONAL AERONAUTICS AND SPACE ADMINISTRATION

Washington, D.C. 20546